# Design Considerations for Microwave Oven Cavities

HAROLD S. HAUCK, MEMBER, IEEE

*Abstract*—**The heating mechanism in a microwave oven results from the interaction of a high-frequency electromagnetic field and the food within it. In most ovens the field is generated by a magnetron which converts dc energy to high-frequency energy at approximately 2450 MHz. This energy is then propagated into the oven chamber which is, in reality, a multimode resonant cavity where the energy is reflected from the walls to create standing wave patterns. To properly design a microwave oven, one must consider not only the magnetron but also the dimensions and resonant properties of the oven cavity. The designer must strive for a uniform energy density within the cavity for uniform cooking of the food and must be sure the cavity presents the proper load to the magnetron. These objectives are discussed, and a procedure for obtaining them is outlined.**

## Modes Within an Oven Cavity

IF WE HAVE a waveguide with the wave propagating along the $Z$ axis as shown in Fig. 1, and then construct two shorting plates as shown, we have created a microwave cavity. This cavity is resonant at a particular set of frequencies. For instance, if the $E$ field varies as shown in Fig. 2, where we have two half-waves in the width direction, three half-waves in the depth direction, and two half-waves in the height direction, the cavity would be resonating in the $TE_{232}$ mode.

The wavelength at which the resonance can occur is given by

$$\lambda = \frac{2}{\sqrt{(M/W)^2 + (N/D)^2 + (P/H)^2}}$$

where $\lambda$ is the wavelength of the resonant frequency; $M$, $N$, and $P$ are the wavenumbers or half-waves of variation of $E$ field in the $W$, $D$, and $H$ directions, respectively; and $W$, $D$, and $H$ are the width, depth, and height of the cavity.

Since energy in a waveguide can propagate in both TE and TM modes, we can have TE and TM resonant modes in a cavity. Thus we will also have a $TM_{232}$ mode, given by the same equation. Since both modes can occur at the same frequency but have different field configurations, they are called degenerate modes. All modes for which the equation holds true can be excited in the cavity except for configurations which violate boundary conditions. These are the $TE_{MNO}$ modes, the $TE_{OOP}$ modes, the $TM_{ONP}$ modes, and the $TM_{MOP}$ modes. Since waveguides will not propagate the TEM mode, this mode is also impossible to sustain in a cavity of this geometry.

Paper 69 TP 64-IGA, approved by the Domestic Appliance Committee of the IEEE IGA Group for presentation at the IEEE 20th Annual Appliance Technical Conference, Detroit, Mich., April 29–30, 1969. Manuscript received August 28, 1969.

The author is with the Amperex Electronic Corporation, Hicksville, N. Y. 11802.

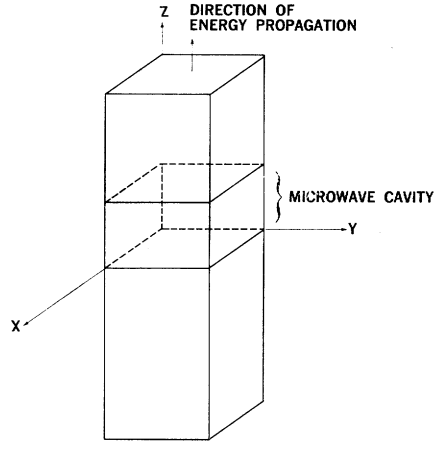


Fig. 1. Waveguide with two shorting plates to form microwave cavity.

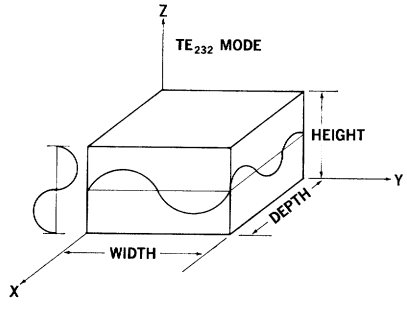


Fig. 2. Microwave cavity formed in Fig. 1 with schematic portrayal of $E$-field variation for the $TE_{232}$ mode.

Because of the field variations due to these modes, areas of high and low energy density will occur in the cavity. If food were placed in such a cavity, it is possible that it may not be cooked uniformly. We have found that cooking uniformly can be increased by, first, choosing dimensions which give the largest number of resonant modes within the frequency limits of the magnetron (2425–2475 MHz); and second, adding a field stirrer to constantly change the energy pattern within the oven.

## Calculation of Modes

A computer program can be written to compute cavity dimensions which have a large number of resonant modes. Essentially, the equation is solved for all combinations of $M$, $N$, and $P$ for small increments of the dimensions, and the combinations which result in a resonant frequency within the desired frequency limits are retained. Two nomographs are also available to facilitate the calculation of modes and cavity dimensions. These nomographs are shown in Figs. 3 [1] and 4 [2] and are described in detail in Appendices I and II. The first nomograph is better for

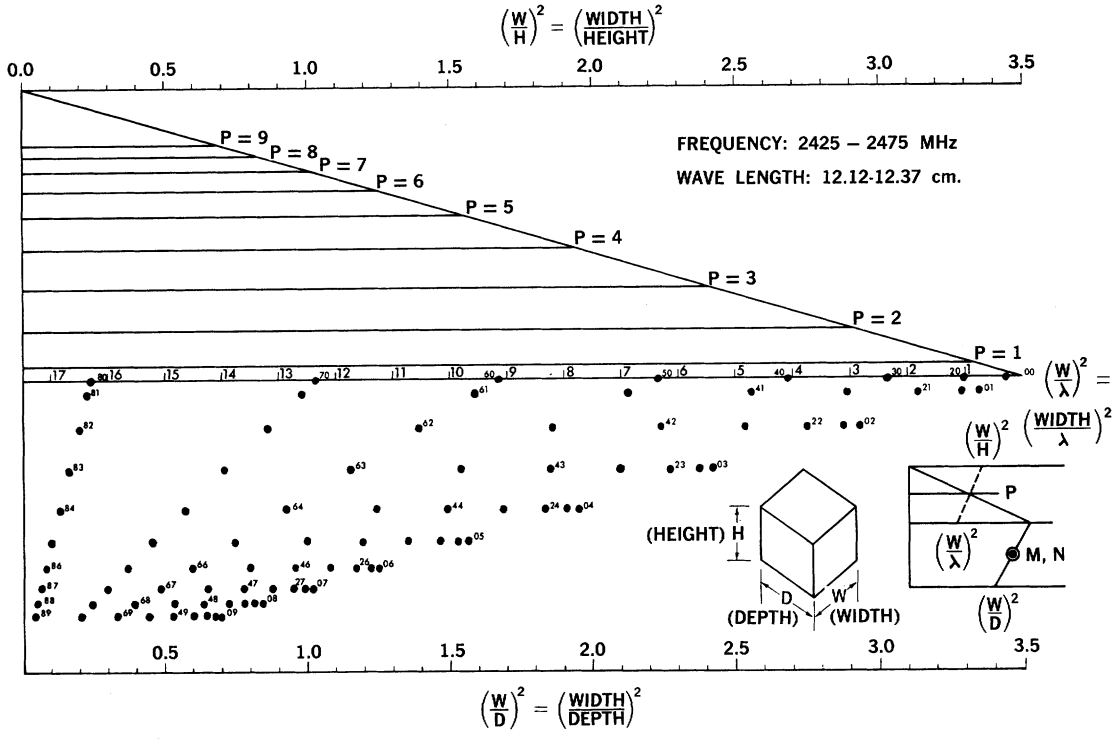


Fig. 3. Nomograph for resonant modes of rectangular microwave oven.

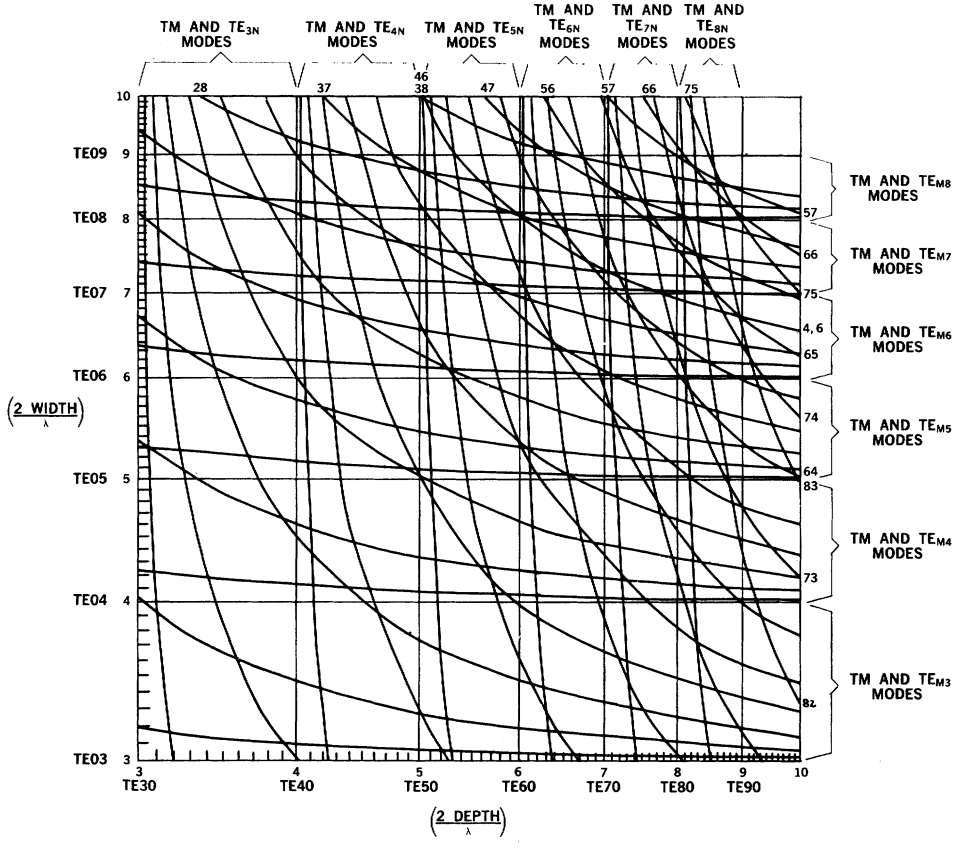


Fig. 4. Mode contours for rectangular cavity; $TE_{MNP}$ and $TM_{MNP}$ modes.

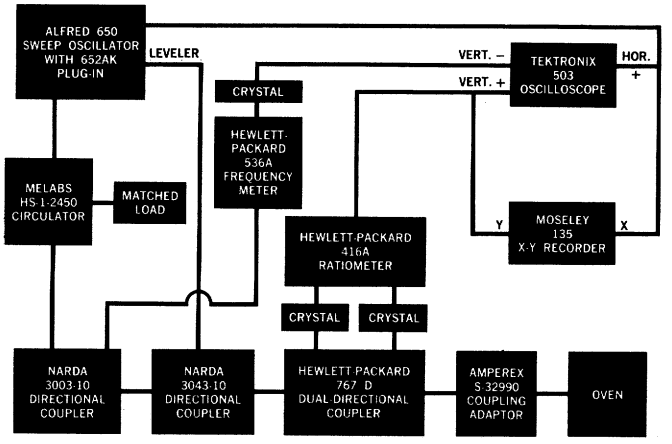


Fig. 5. Sweep frequency test circuit.

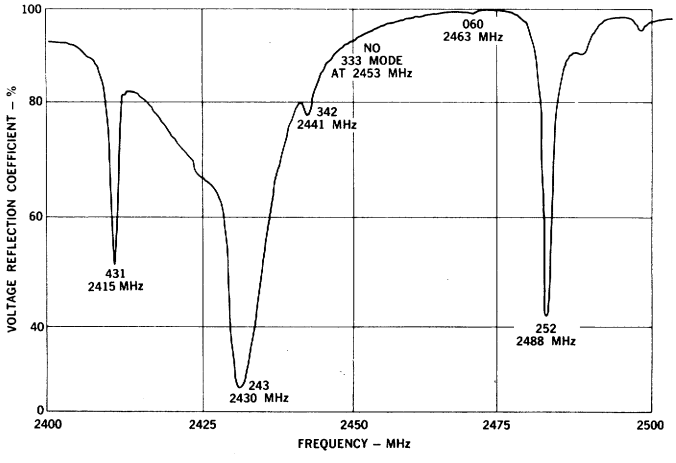


Fig. 6. Voltage reflection coefficient versus frequency showing resonant modes in oven cavity with width 29.7 cm, depth 36.6 cm, and height 30.2 cm.

calculating modes in a cavity of known dimensions, while the second nomograph is better for calculating dimensions which will have a large number of modes.

To verify the existence of these modes, we calculated the modes for a cavity with width of 29.7 cm, depth of 36.6 cm, and height of 30.2 cm.

| Mode | Frequency (MHz) |
|---|---|
| 431 | 2415 |
| 243 | 2430 |
| 342 | 2441 |
| 333 | 2453 |
| 060 | 2462 |
| 252 | 2488 |

The cavity was then tested using the circuit of Fig. 5.

In the system we used the sweep oscillator to vary the frequency from 2400 to 2500 MHz; a dual directional coupler to sample the energy coming from the oscillator and the energy being reflected from the cavity; and the ratiometer to convert the two signals to the amplitude of the voltage reflection coefficient. This is a measure of the ratio of reflected to incident energy. The output from the ratiometer can be fed into either an oscilloscope or an $X$–$Y$ recorder.

Fig. 6 shows the results using an $X$–$Y$ recorder. At a resonant frequency, energy will be absorbed by the cavity and will not be reflected. At a frequency which is not resonant, the energy will be reflected. As seen in the figure, we have resonances occurring at approximately the calculated frequencies for the 431, 243, 342, and 252 modes. We do not see the 333 mode, and we have a slight trace of the 060 mode. We do have evidence of 2 additional modes near 2500 MHz. Possibly these are due to resonances within the coupling system, or they might be the appearance of higher frequency modes caused by our errors in measuring the cavity. The figure shows that most, but not necessarily all, of the calculated modes will appear in the cavity. Whether or not a mode appears is largely determined by the manner in which the energy is coupled into the cavity.

## Field Stirrer

The mode pattern within the cavity can be continually disturbed by adding a field stirrer, which is a bladed device similar to a fan and which rotates at a frequency which should be asynchronous with the 60-Hz power frequency. The effect of a stirrer can be seen in Fig. 7, which shows the heating pattern for an oven cavity with and without a stirrer. The patterns were obtained by placing a layer of moistened silica gel in the cavity and operating the magnetron to see how uniformly the silica gel dries. Silica gel is normally used as a desicant and is light pink when moist but turns various shades of blue as it becomes dry. The light areas in the figure show areas which were not being heated by the energy within the oven. As seen in the figure, the uniformity of heating was improved by the field stirrer.

As a demonstration of what is actually happening in the cavity as the stirrer rotates, we took pictures of the heating pattern for six consecutive 2-degree increments of rotation of the stirrer. These are shown in Fig. 8. A close examination of the figure will show that the areas of high and low energy density appear and disappear, and that, at the same time, the areas appear to move around slightly within the oven. A further demonstration of what is happening is given in Fig. 9, showing $X$–$Y$ recorder traces of voltage reflection coefficient versus frequency for the 2-degree increments of stirrer rotation. The figure shows the modes appearing and disappearing, and at the same time, changing frequency slightly. The changes in frequency suggest that the stirrer changes the effective dimensions of the cavity as it rotates.

## Load Presented to the Magnetron

Fig. 10 shows a magnetron operating into a transmission line which is terminated in a load. If the load has the same impedance as the transmission line, the load is said to be matched, and will absorb all the energy propagating to it.

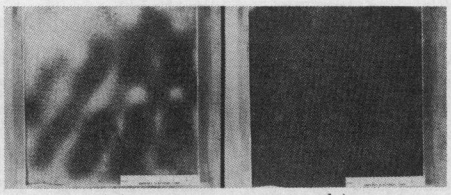

(a) (b)

Fig. 7. Silica gel patterns. (a) Without stirrer. (b) With stirrer.

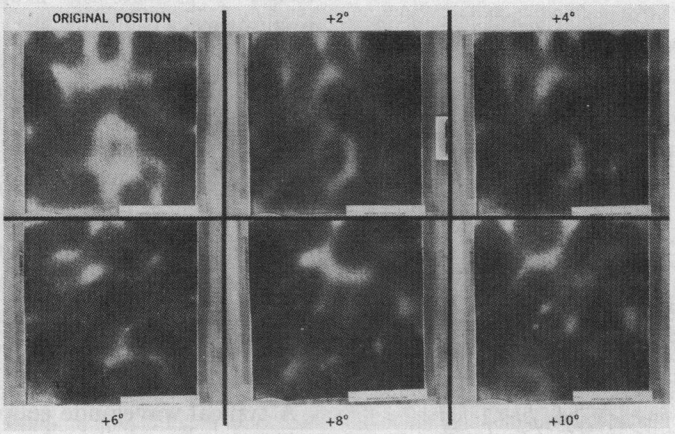


Fig. 8. Silica gel patterns; six consecutive 2-degree turns of stirrer in cavity.

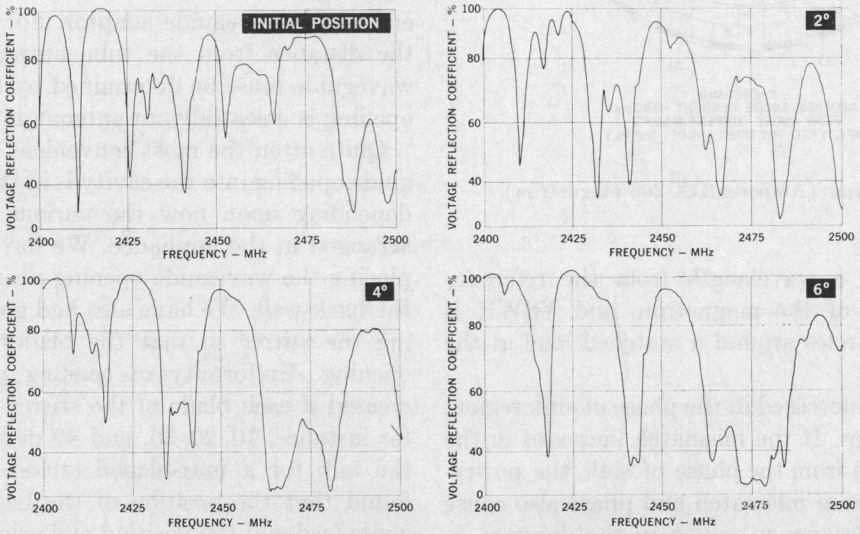


Fig. 9. Voltage reflection coefficient versus frequency; four consecutive 2-degree turns of stirrer in cavity.

If the load does not have the same impedance as the line, the existing mismatch will cause part of the energy to be reflected, the amount of energy reflected being determined by the degree of mismatch. As a manifestation of this reflected energy, a standing wave pattern, shown schematically in the figure, will be created on the transmission line. This can be characterized by the voltage standing wave ratio, which is the ratio of the voltage at the maximum to the voltage at the minimum of the standing wave pattern, and by the position of the minimum expressed in wavelengths from the reference plane at the output of the magnetron. It can also be characterized by the magnitude and phase of the voltage reflection coefficient mentioned earlier. Changes in the load at the end of the transmission line will result in changes in the magnitude and phase of the standing wave pattern. The effect of these variations is shown in the load diagram of Fig. 11. Contours of constant power output and constant frequency are plotted versus magnitude and phase of the voltage standing wave ratio. The phase is

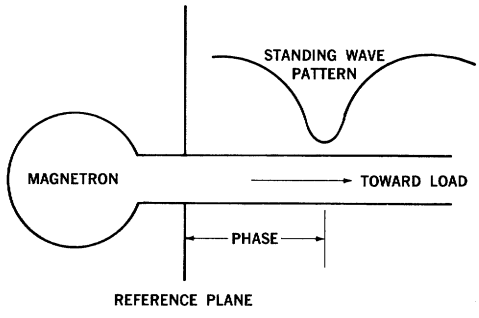


Fig. 10. Magnetron operated into a transmission line.

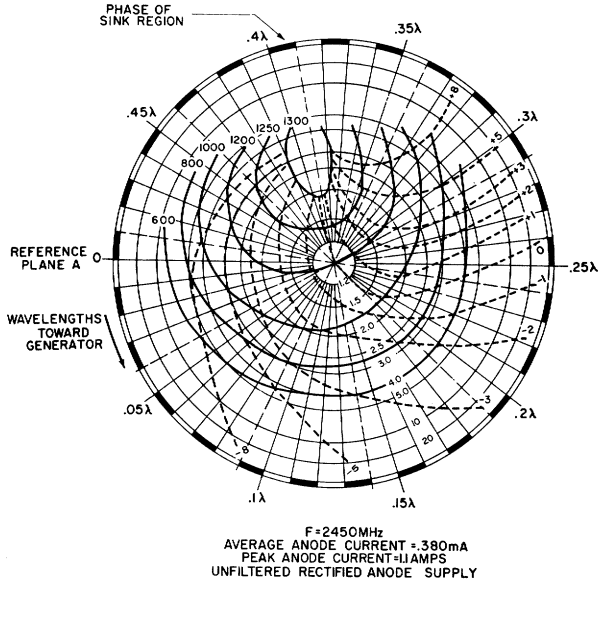


Fig. 11. Load diagram (Amperex DX-206 magnetron).

given in fractions of a wavelength from the reference plane at the output of the magnetron, and VSWR is given by concentric circles around a matched load at the center of the diagram.

As the mismatch is increased in the phase of sink region, the power-out increases. If the mismatch increases in the region 1/4 wavelength from the phase of sink, the power-out decreases. Changes in mismatch and phase also cause changes of the tube frequency, given in the diagram as deviations in MHz from the frequency at a matched load.

For proper operation of the magnetron, the oven cavity should present as near a matched load as possible. If mismatches do occur it is desirable that they be near the phase of sink region at the center frequency of the cooking band (2450 MHz).

## Design of Oven Cavity

The oven cavity should have a good heating pattern and should present the proper load to the magnetron. Although the method for obtaining these results is more of an art than a science at the present time, definite procedures can be recommended. The first step is to obtain the proper oven dimensions. The rough range of dimensions will probably be dictated by constraints other than electrical, such as the overall size of the appliance and the types of foods to be cooked. The final dimensions within these rough limits should give as large a distribution of resonant modes within the range of 2425 to 2475 MHz, since the larger the number of modes the larger the probability of coupling these modes into the cavity. It is then necessary to obtain a coupling system, including the location of the coupling into the oven cavity, and a stirrer design to present the proper VSWR and phase to the magnetron.

To facilitate our work we use the test setup shown in Fig. 5. With this equipment we can change the cavity design parameters at will and immediately see its effect on the magnitude of the voltage reflection coefficient. The coupling adaptor in Fig. 5 allows the equipment to "see" the oven cavity as the magnetron will see it. It is possible to make single-frequency measurements using the equipment of Fig. 12, but the procedures are more time consuming. More sophisticated equipment showing both magnitude and phase of voltage reflection coefficient is also available.

A typical waveguide coupler using a 2- by 4-inch waveguide to transmit the energy from the magnetron to the oven cavity is shown in Fig. 13. The opening into the cavity is 2 by 4 inches, and the center of the opening for the magnetron output is 1.171 inches from the opposite end of the waveguide adaptor. For other size waveguides the distance from the tube output to the back of the waveguide must be determined by trial. The 2- by 4-inch opening is essentially an antenna into the oven cavity.

Quite often the most convenient location for the waveguide opening into the cavity is in the top or the back wall, depending upon how the various components must be arranged in the appliance. We have had good results by placing the waveguide opening near one of the corners of the back wall. We have also had good results by positioning the stirrer so that the blades pass in front of the opening. Uniformity of cooking pattern is usually increased if each blade of the stirrer is at a different pitch, for instance, 10, 20, 30, and 40 degrees from the plane of the hub for a four-bladed stirrer. In general, we have found that the position of the back plate of the waveguide feed and the position and orientation of the opening affect, mostly, the magnitude of the VSWR; the length of the waveguide feed affects the phase; and the stirrer design affects the uniformity of cooking.

When the position and orientation of the antenna opening and the stirrer design have been adjusted to give the best matched load over the frequency range, it is then necessary to measure the phase and VSWR at single frequencies, say 2425, 2450, and 2475 MHz. We normally measure at 16 uniformly spaced positions of the stirrer blade at each frequency. From these measurements one can tell whether the length of the waveguide coupler must be adjusted to put the phase of the load, represented by the cavity, in the best location with respect to the magnetron reference plane.

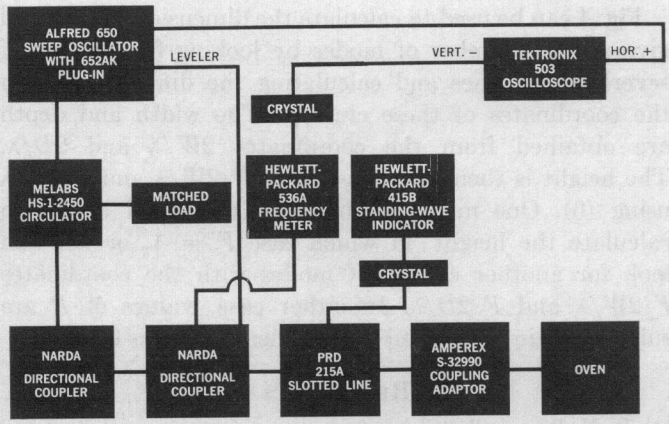


Fig. 12. Single-frequency test circuit.

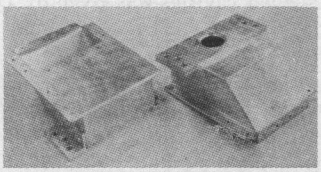

Fig. 13. Typical waveguide coupler used to direct energy from Amperex DX-206 magnetron to oven cavity.

When the oven cavity has been properly adjusted using the test instrumentation, the magnetron can then be attached and operated to determine the uniformity of heating. This can be done using the silica gel technique described earlier and by spacing various foods at regular intervals throughout the oven. A good test of pattern uniformity is to bake a cake in the oven. With a poor pattern, the cake will rise unevenly. If the pattern is not sufficiently uniform, adjustments in the stirrer and possibly the opening position and orientation must be made. This being the case, the oven will then have to be reevaluated to be sure it still presents the proper load to the magnetron. When the VSWR, phase, and pattern are satisfactory, the design of the cavity and coupling are complete. The objectives of good heating uniformity and proper load for the magnetron will have been obtained.

## Conclusion

Careful design of the oven cavity following the procedures outlined will give optimum operation of the magnetron and will lead to more efficient cooking. The techniques which have been given closely follow theoretical considerations and give excellent results.

## Appendix I

The nomograph of Fig. 3 can be used as indicated by the example in the lower right corner of the figure.

1) The ratios $(W/H)^2$ = (width/height)$^2$, $(W/\lambda)^2$ = (width/wavelength)$^2$, and $(W/D)^2$ = (width/depth)$^2$ must be calculated using both wavelengths, 12.12 and 12.37 cm, corresponding to 2475 and 2425 MHz, respectively.

2) Draw lines from $(W/H)^2$ on the upper scale to both values of $(W/\lambda)^2$ on the center scale corresponding to the $P = 0$ line.

3) Draw lines from both values of $(W/\lambda)^2$ on the center scale to the value of $(W/D)^2$ on the bottom scale. All dots in the lower portion of the nomograph occurring within this wedge correspond to modes with $P = 0$ occurring within the wavelength limits 12.12 to 12.37 cm.

4) Draw lines from the origin of the $(W/H)^2$ axis through the intersection of the lines of step 2) with the $P = 1$ line to the center scale. Connect these newly obtained points on the center scale with $(W/D)^2$ on the lower scale. All crosses within the new wedge correspond to modes with $P = 1$.

5) Repeat step 4) using the $P = 2$ line to obtain modes with $P = 2$. This step is then repeated for all $P$ lines crossed by the lines of step 2).

## Appendix II

In [2] Griemsmann gave a graph for determining modes in an oversized waveguide. Using the equation

$$\frac{M^2}{(2W/\lambda)^2} + \frac{N^2}{(2D/\lambda)^2} = 1 = \frac{1}{\sec^2\theta} + \frac{1}{\csc^2\theta} \tag{1}$$

where $W$ and $D$ are the transverse dimensions of the waveguide and $M$, $N$, and $\lambda$ are given in Fig. 2, he obtained the parametric equations

$$\frac{2W}{\lambda} = M \sec\theta \quad \text{and} \quad \frac{2D}{\lambda} = N \csc\theta. \tag{2}$$

These were used to obtain the plot of $2D/\lambda$ versus $2W/\lambda$ for all TE and TM modes with mode numbers up to 5, covering the range $1 \leq 2D/\lambda \leq 10$ and $1 \leq 2W/\lambda \leq 10$. The plotting points for the graph were obtained by choosing values of $M$, $N$, and $\theta$ to satisfy the equations

$$1 \leq M \sec\theta \leq 10 \quad \text{and} \quad 1 \leq N \csc\theta \leq 10. \tag{3}$$

For our work we constructed a similar but larger graph covering the range of $2W/\lambda$ and $2D/\lambda$ from 3 to 10, and including modes with mode numbers up to 8. Fig. 4 is the resulting graph. Each curve represents a mode or pair of degenerate modes as indicated around the periphery.

To use the graph for calculations of rectangular cavities, (1) can be modified as follows. Consider the equation for rectangular cavities:

$$\frac{M^2}{(2W/\lambda)^2} + \frac{N^2}{(2D/\lambda)^2} + \frac{p^2}{(2H/\lambda)^2} = 1. \tag{4}$$

This can be rewritten as

$$\frac{M^2}{(2W/\lambda)^2} + \frac{N^2}{(2D/\lambda)^2} = 1 - \frac{p^2}{(2H/\lambda)^2} \equiv F^2$$

or

$$\frac{M^2}{(F\cdot 2W/\lambda)^2} + \frac{N^2}{(F\cdot 2D/\lambda)^2} = 1 \tag{5}$$

where

$$F = \left[1 - \frac{P^2}{(2H/\lambda)^2}\right]^{1/2} = \tanh\left[\cosh^{-1}\left(\frac{2H}{P\lambda}\right)\right]. \tag{6}$$

To calculate the modes in a cavity, we must thus calculate the factor $F$ from (6) from the height $H$ of the cavity and the mode number $P$. $F$ can then be substituted into (5) to obtain the quantities $F\cdot 2W/\lambda$ and $F\cdot 2D/\lambda$. To enter the graph, the graph can be used with either set of coordinates $2W/\lambda\cdot 2D/\lambda$ or $(F\cdot 2W/\lambda)\cdot(F\cdot 2D/\lambda)$. As in the case of Fig. 2, the modes which fall within the wavelength range of 12.12–12.37 cm are the cavity modes of interest.

Fig. 4 can be used to calculate the dimensions which will give a large number of modes by looking for clusters of several mode lines and calculating the dimensions from the coordinates of these clusters. The width and depth are obtained from the coordinates $2W/\lambda$ and $2D/\lambda$. The height is then calculated from $F\cdot 2W/\lambda$ and $F\cdot 2D/\lambda$ using (6). One may use the same cluster of modes to calculate the height, in which case $F = 1$, or one can look for another cluster of modes with the coordinates $F\cdot 2W/\lambda$ and $F\cdot 2D/\lambda$. In either case, values of $P$ are substituted into (6) until a convenient height is obtained.

## References

[1] R. N. Bracewell, "Charts for resonant frequencies of cavities," *Proc. IRE* (Waves and Electrons), vol. 35, pp. 830–841, August 1947.

[2] J. W. E. Griemsmann, "Oversized waveguides," *Microwaves*, vol. 2, pp. 20–31, December 1963. (The method for using the graph for rectangular cavities was given by Dr. Griemsmann in private correspondence.)

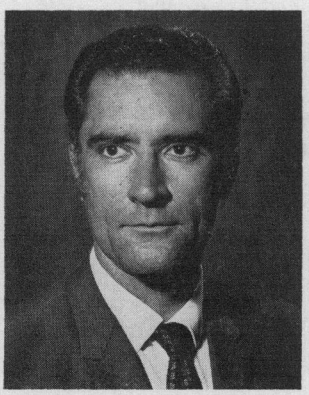

**Harold S. Hauck** (M'56) was born on November 3, 1931. He received the A.B. degree in mathematics and the M.S. degree in engineering from the University of Pennsylvania, Philadelphia, in 1954 and 1964, respectively. He is presently working toward the M.S. degree in industrial management at the Polytechnic Institute of Brooklyn, Brooklyn, N. Y.

Upon graduation in 1954 he joined the Research Laboratory of the Polymer Corporation, where he was responsible for research into the dielectric, dynamic mechanical, and frictional properties of plastics. While there, he developed a filled-plastic magnetic material for use in RF, UHF, and microwave circuits. In 1961 he joined the Plastics Engineering Laboratory of Rohm and Haas Company. His principle duties were to study the plate and shell properties of structures made from acrylic plastics for architectural applications. Since 1966 he has been employed by the Amperex Electronic Corporation, Hicksville, N. Y., in the areas of magnetron development and applications research and assistance in microwave oven design.